



J/ψ, Y, χ_b(3P) production with the ATLAS Detector

Rui Wang

University of New Mexico

on behalf of the ATLAS collaboration

Outline

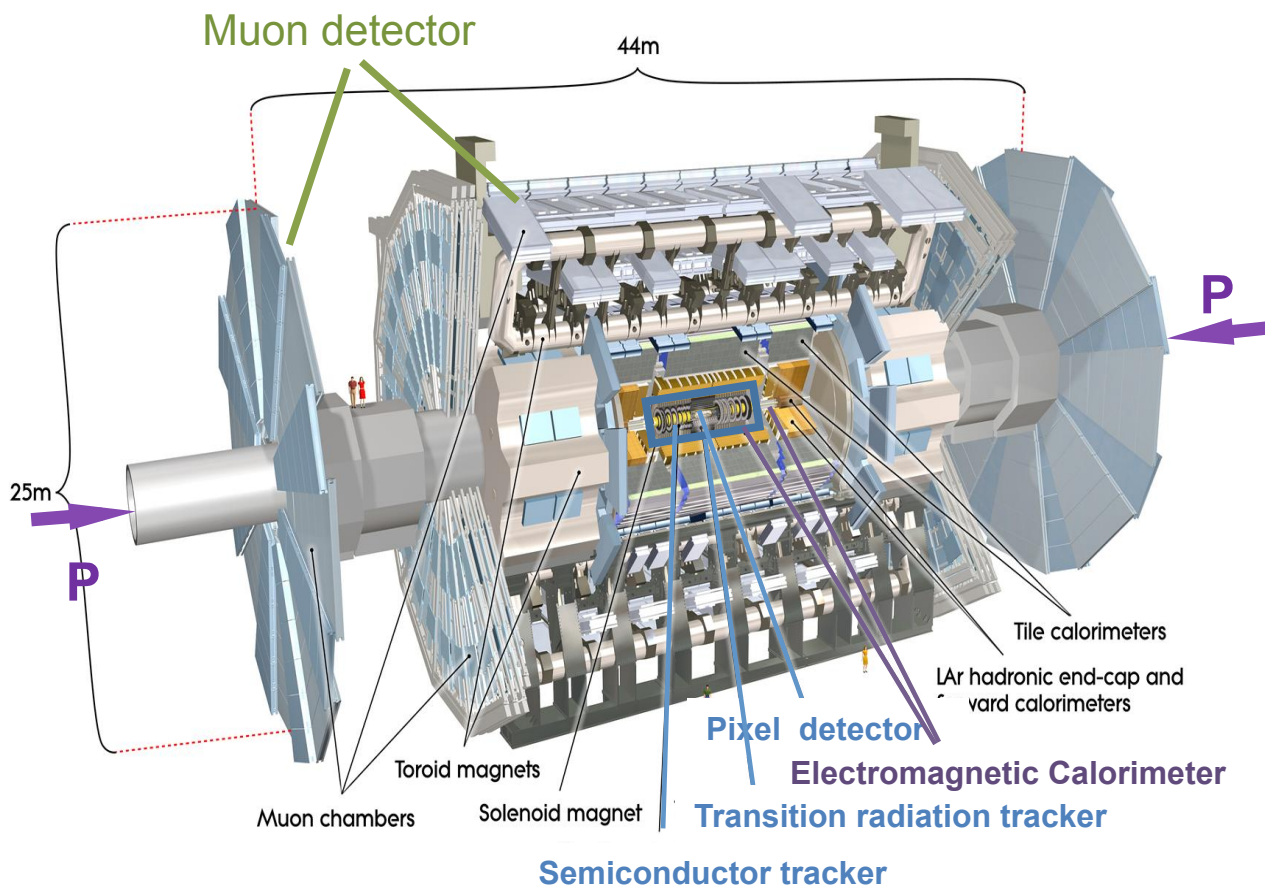
- Introduction of ATLAS detector.
- Muon reconstruction.
- Measurement of the differential cross-sections of J/ψ .
- Measurement of the $\Upsilon(1S)$ production cross-section.
- Observation of a new χ_b state in radiative transitions to $\Upsilon(1S)$ and $\Upsilon(2S)$.

ATLAS public results:

- Measurement of the differential cross-sections of inclusive, prompt and non-prompt J/ψ production in proton–proton collisions at $\sqrt{s} = 7 \text{ TeV}$
([Nuclear Physics B 850 \(2011\) 387–444](#))
- Measurement of the $\Upsilon(1S)$ production cross-section in pp collisions at $\sqrt{s} = 7 \text{ TeV}$ in ATLAS ([Physics Letters B 705 \(2011\) 9–27](#))
- Observation of a new χ_b state in radiative transitions to $\Upsilon(1S)$ and $\Upsilon(2S)$ at ATLAS
([arXiv:1112.5154v5 \[hep-ex\] 11 Apr 2012](#))

ATLAS detector

The ATLAS detector consists of **Inner detector**(Pixel, SCT and TRT), EM calorimeter, Hadronic calorimeter and **Muon detector**.



Inner detector, $|\eta| < 2.5$.

Momentum resolution:
 $\sigma/p_T \sim 3.8 \times 10^{-4}/p_T(\text{GeV}) + 0.015$.

Primary vertex resolution:
 $\sim 30 \mu\text{m}$ transverse, $\sim 50 \mu\text{m}$ longitudinal.

EM calorimeter, $|\eta| < 3.2$

E-resolution: $\sigma/E \sim 10\%/\sqrt{E} (\text{GeV})$.

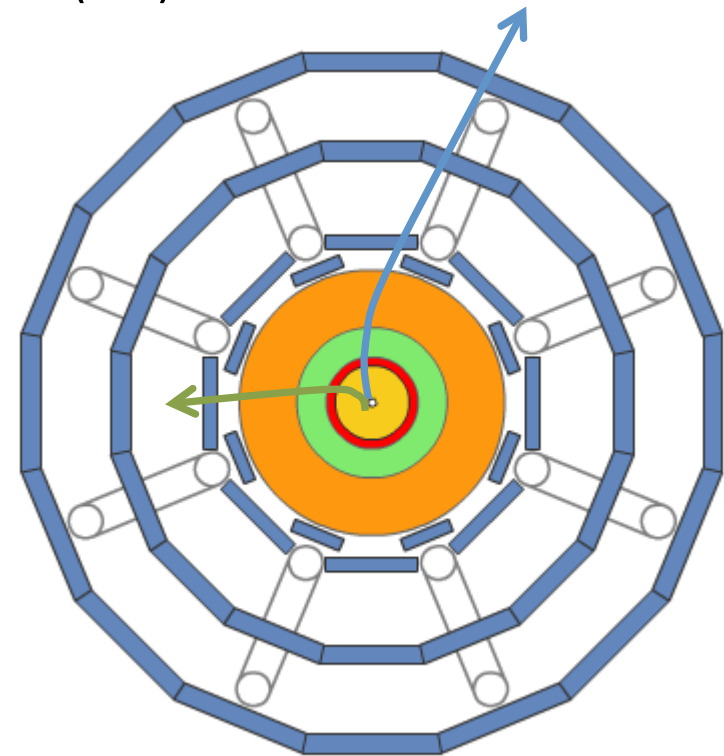
Muon Spectrometer,
 $|\eta| < 2.7$

Momentum resolution: $\sigma/p_T \sim 10\%$ at $E_\mu = 1 \text{ TeV}$.

Muon reconstruction

The muon reconstruction in ATLAS makes use of two sub-detectors: the Inner Detector (ID) and the Muon Spectrometer (MS).

- **Combined muons**: a stand-alone MS track ($|\eta| < 2.5$) matched with an ID track.
- **Tagged muons**: ID tracks extrapolated to the MS and matched to at least one of MS hits.



Triggers

B-physics starts with single or Di-muon triggers with various thresholds:

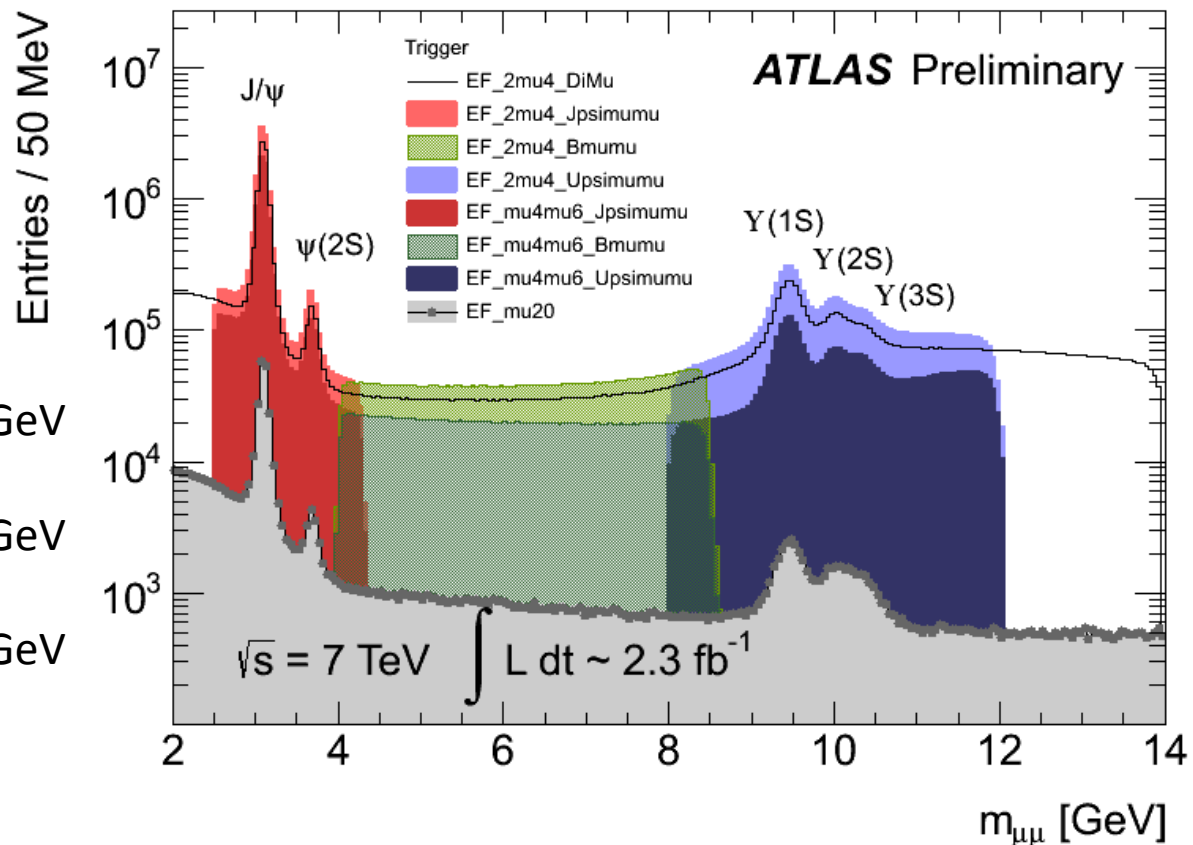
$p_T(\mu) > 6 \text{ GeV}$

$p_T(\mu) > 18 \text{ GeV}$

$p_T(\mu_1) > 4 \text{ GeV} \& p_T(\mu_2) > 4 \text{ GeV}$

$p_T(\mu_1) > 6 \text{ GeV} \& p_T(\mu_2) > 4 \text{ GeV}$

$p_T(\mu_1) > 6 \text{ GeV} \& p_T(\mu_2) > 6 \text{ GeV}$



Di-muon mass range: $m(\mu\mu) \in [2.5; 4.3] \text{ GeV}$ (final states containing J/ψ), $m(\mu\mu) \in [4.0; 8.5]$ GeV (B to μ transitions) and $m(\mu\mu) \in [8.0; 12.0]$ for Y region.

Measurement of the differential cross-sections of inclusive, prompt and non-prompt J/ψ production in proton–proton collisions at $\sqrt{s} = 7\text{ TeV}$

Measurement of J/ψ cross-sections

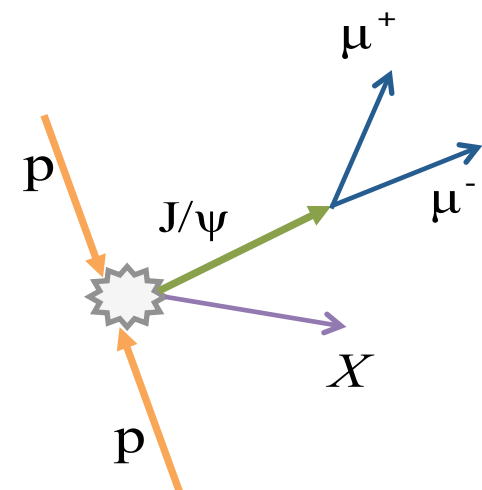
- Results were obtained using 2.2 pb⁻¹ of data obtained using the ATLAS detector in 2010.
- Inclusive J/ψ production: $pp \rightarrow J/\psi X$
 - non-prompt J/ψ's: $pp \rightarrow B X \rightarrow J/\psi X'$
$$f_B \equiv \frac{\sigma(pp \rightarrow B + X \rightarrow J/\psi X')}{\sigma(pp \xrightarrow{\text{Inclusive}} J/\psi X'')}$$
 - prompt J/ψ's: $(1-f_B)$
- Measured as a function of J/ψ's p_T and y.
- Results are compared to various theoretical predictions.

Trigger, events and candidates selection

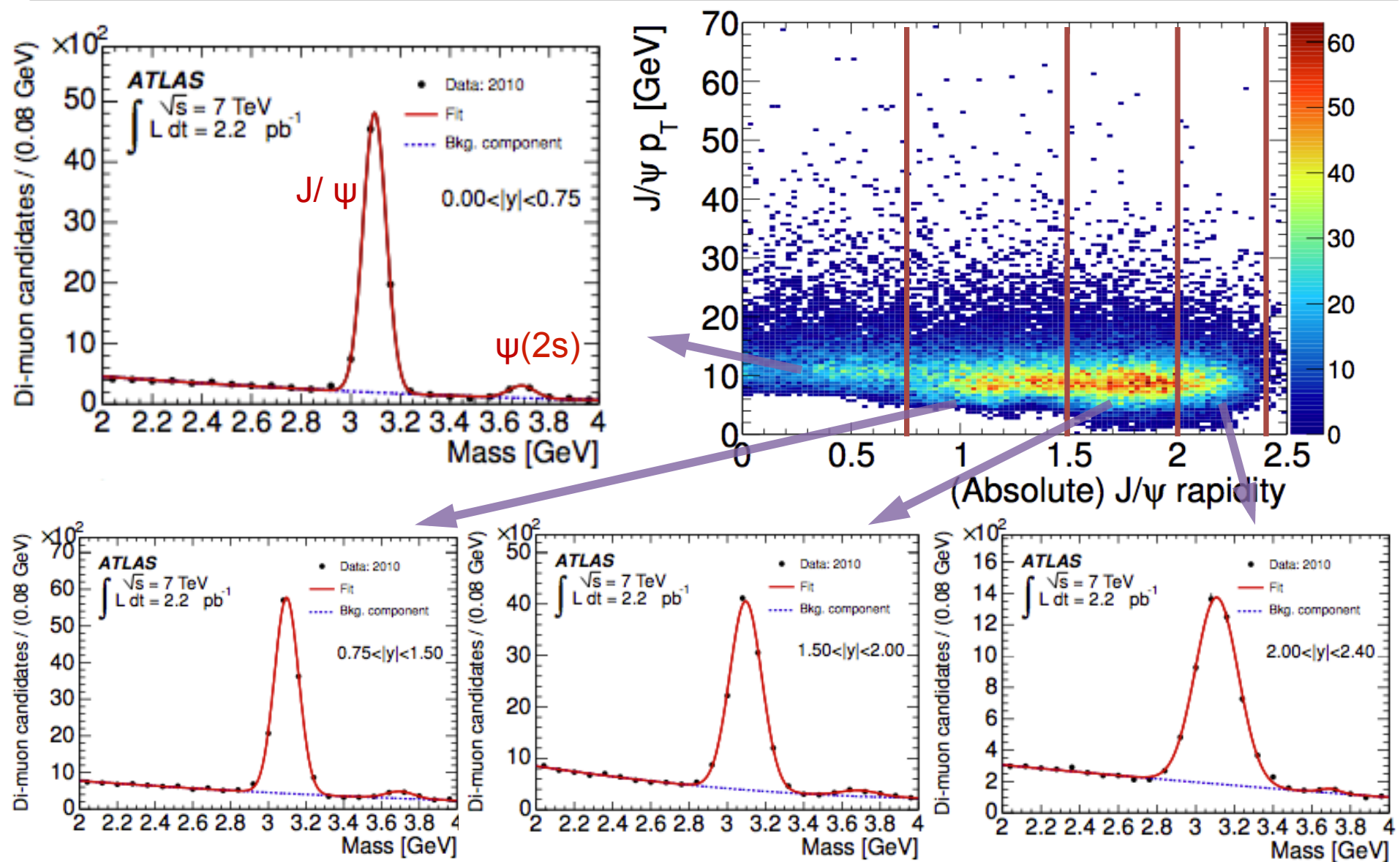
- Trigger:
 - In this measurement, the trigger relies on the Minimum Bias Trigger.
 - With the increase of the instantaneous luminosity:

$$p_T(\mu) > 4 \text{ GeV} \rightarrow p_T(\mu) > 6 \text{ GeV}$$

- Selection criteria:
 - Opposite charged Di-muon pair reconstructed in the event.
 - At least 3 tracks associated with primary vertex.
 - At least one muon to be Combined in Di-muon pair.
 - Tracks: Pixel hits > 0, SCT hits > 5
 - Very loose J/ ψ vertex quality requirement (vertex fit χ^2 per number degree of freedom < 200)

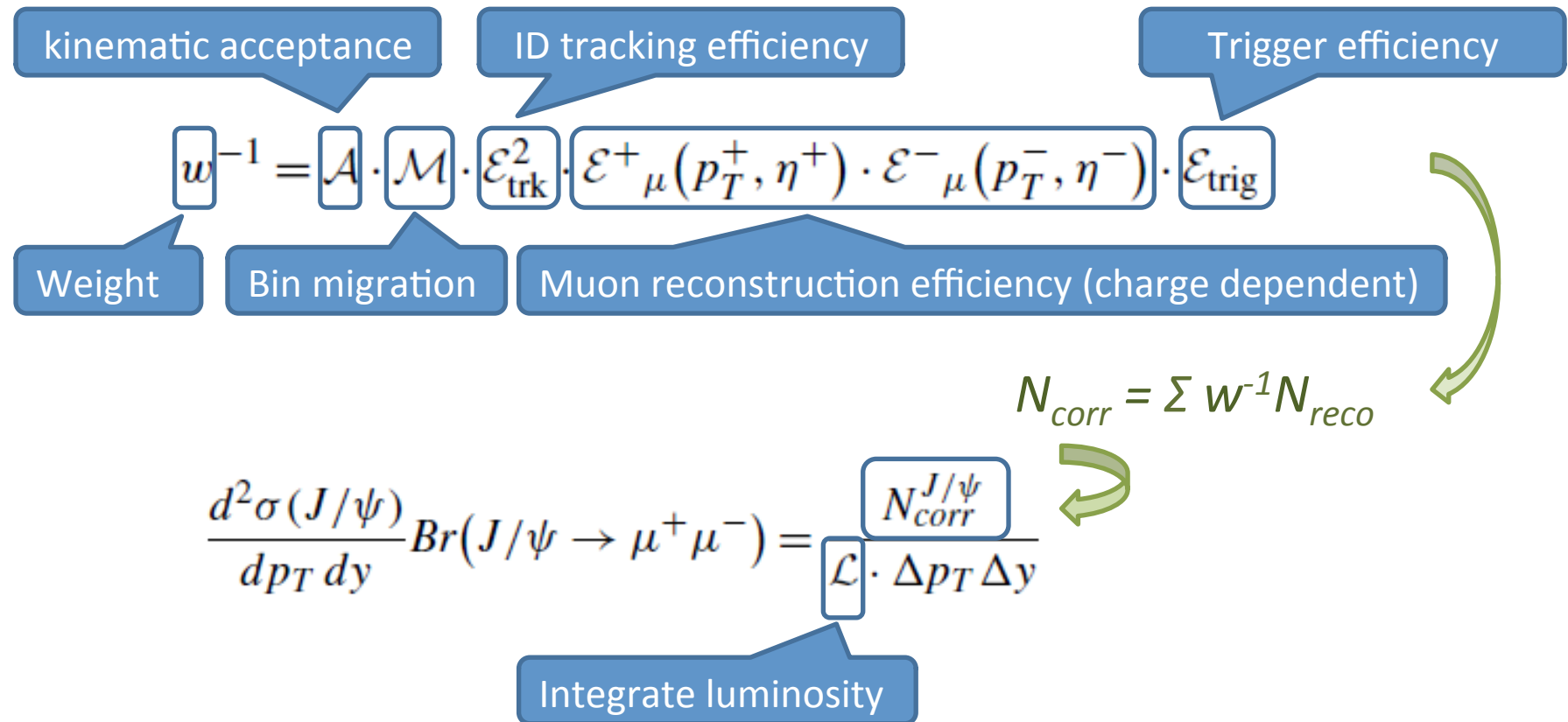


Inclusive J/ψ in $\{p_T, y\}$



Differential cross-sections of inclusive J/ψ production

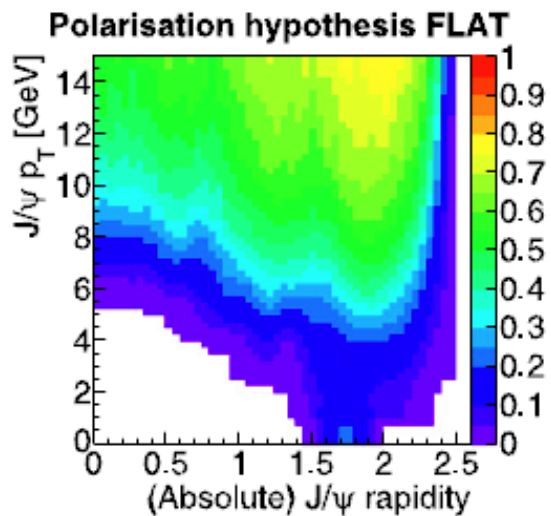
- Reconstruct J/ψ candidates in $p_T - y$ bins.
- The probability that a $J/\psi \rightarrow \mu\mu$ decay is reconstructed depends on the kinematics acceptance, bin migration, ID tracking efficiency, muon reconstruction efficiency and trigger efficiency.



Inclusive J/ ψ production: Acceptance, Bin Migration and Efficiencies

Acceptance : probability of $J/\psi(p_T, y)$ decays fall into certain active region of the detector.

- Using generator-level Monte Carlo.
- Dependent on spin alignment.



Bin Migration: due to detector resolution, MC J/ψ candidates identified to incorrect $p_T - y$ bin before smearing.

- smearing with ATLAS muon resolution, ratio is assigned to be the correct factor.
- 0.1%-3%, increasing with p_T and y .

ID track efficiency: $99.5\% \pm 0.5\%$ per track.

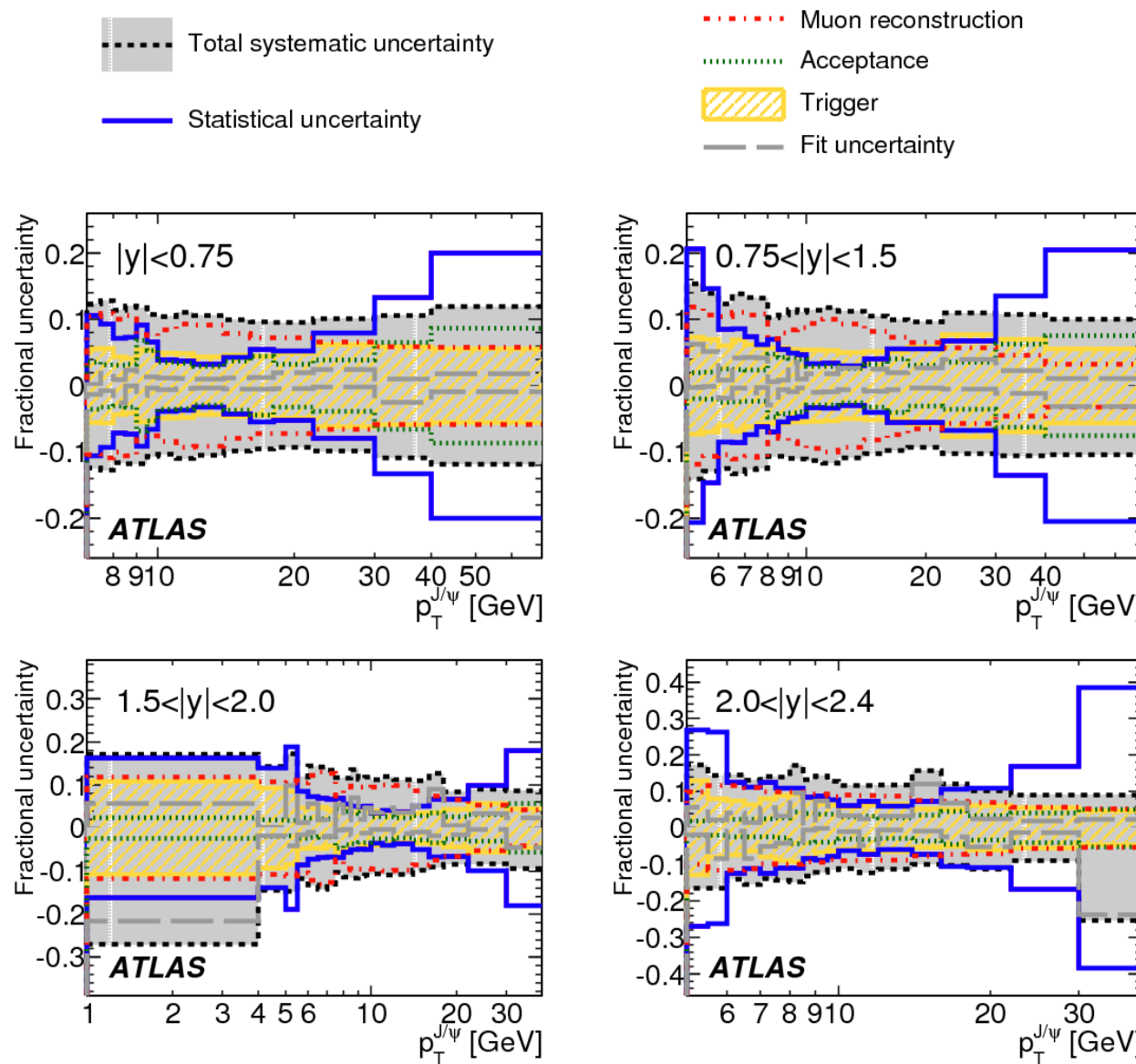
Muon reconstruction efficiency: obtained from data (Tag & Probe) using J/ψ (low p_T) and Z (high p_T) decay (20%-98%).

Trigger efficiency: obtained from Monte Carlo and then corrected by data (Tag & Probe) for both positive and negative muons. (80% in barrel, 95% in endcap)

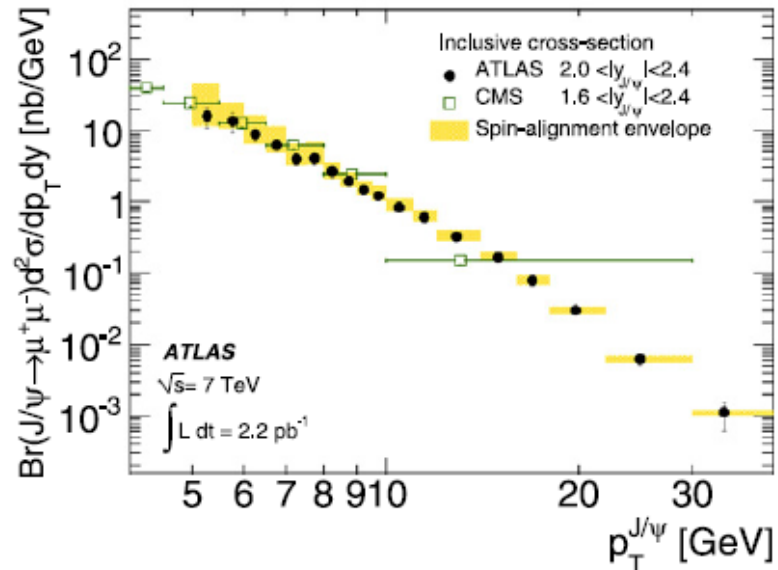
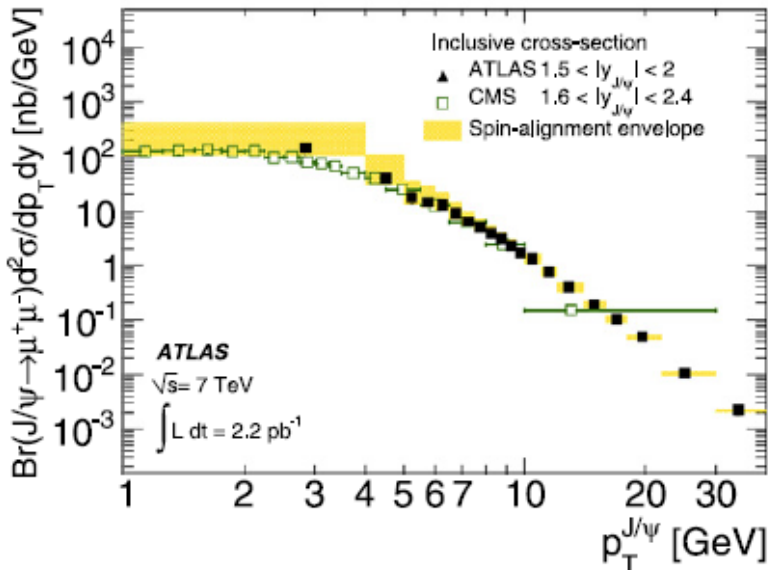
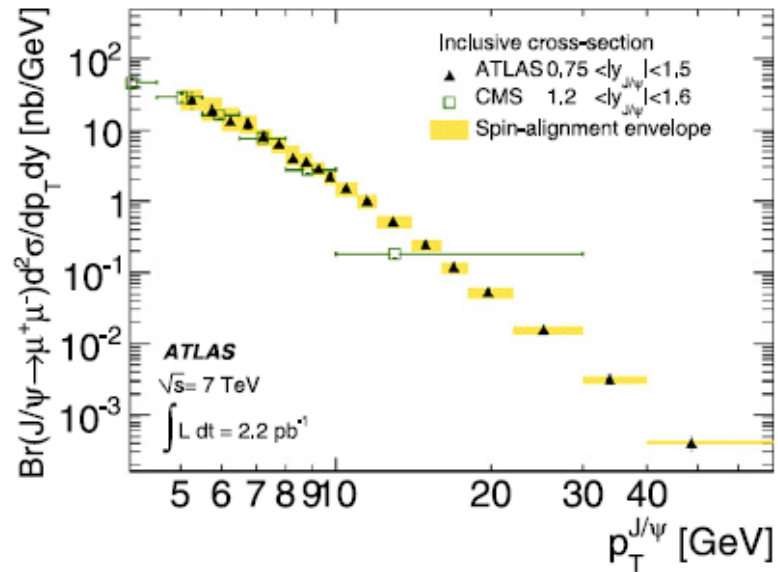
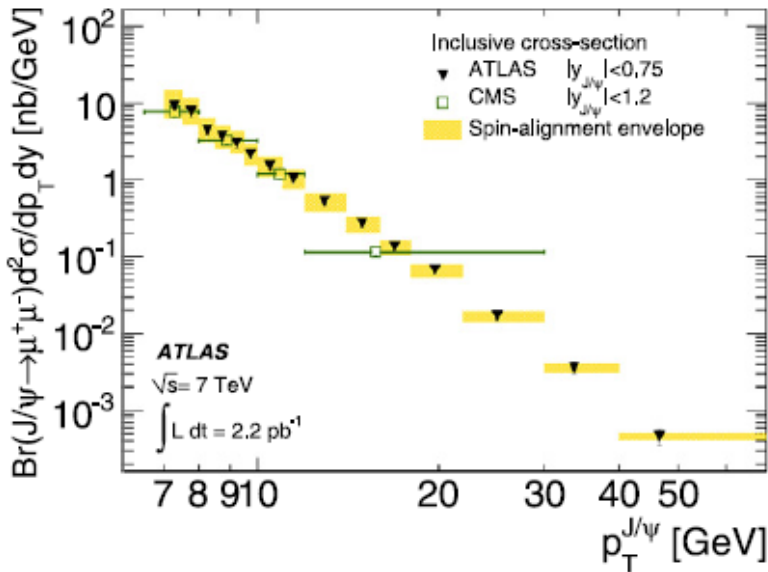
Inclusive J/ ψ production: systematic uncertainties

- Spin alignment: In each bin, the maximal deviations in either direction due to the unknown J/ ψ spin alignment are assigned as the systematic uncertainty.
- Muon reconstruction efficiency: Uncertainties from the Tag & Probe method, 5% - 10%.
- ID track efficiency: 0.5%, added linearly.
- Trigger efficiency: Uncertainties from the Tag & Probe method and reweighting of MC maps to the data-driven efficiency values, \sim 5%.
- Luminosity: 3.4%.
- Acceptance: From MC statistics, \sim 1 to 2%.
- Bin migration: By smearing the efficiency and acceptance corrected p_T spectrum with a Gaussian resolution function (width based on muon p_T resolutions in data), 0.1% - 3%.
- Kinematic dependence: Variation of MC spectra and slight differences between prompt and non-prompt components, $<$ 1.5%.
- Final State Radiation: $<$ 0.1%.
- Fit: variations in fitting models include signal and background fitting functions and inclusion/exclusion of the $\psi(2S)$ regime, 1%(low p_T and y) - 3%(high p_T and y).
- J/ ψ vertex finding efficiency: negligible.

Inclusive J/ψ production: systematic uncertainties



Cross-sections of inclusive J/ ψ production



Cross-sections of inclusive J/ψ production

The total cross-section for inclusive $J/\psi \rightarrow \mu^+\mu^-$ production, multiplied by the branching fraction into muons and under the “FLAT” production scenario:

- J/ψ produced within $|y| < 2.4$ and $p_T > 7$ GeV, maximum range of y .

$$Br(J/\psi \rightarrow \mu^+\mu^-)\sigma(pp \rightarrow J/\psi X; |y_{J/\psi}| < 2.4, p_T^{J/\psi} > 7 \text{ GeV}) \\ = 81 \pm 1(\text{stat.}) \pm 10(\text{syst.}) \pm 25(\text{spin}) \pm 3(\text{lumi.}) \text{ nb}$$

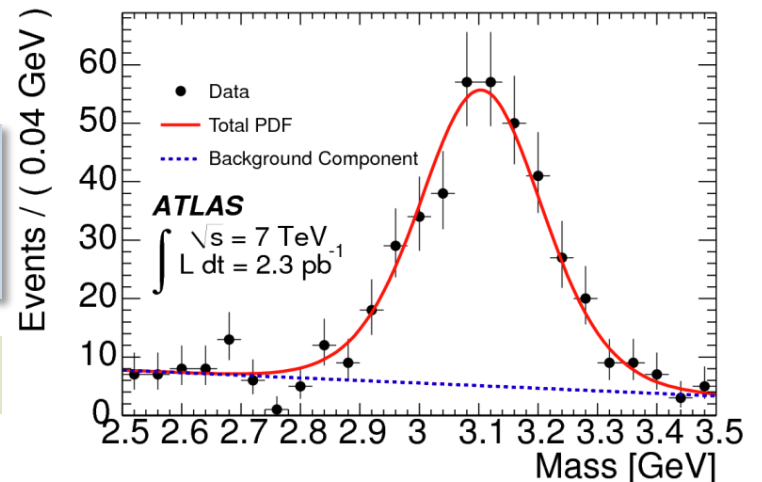
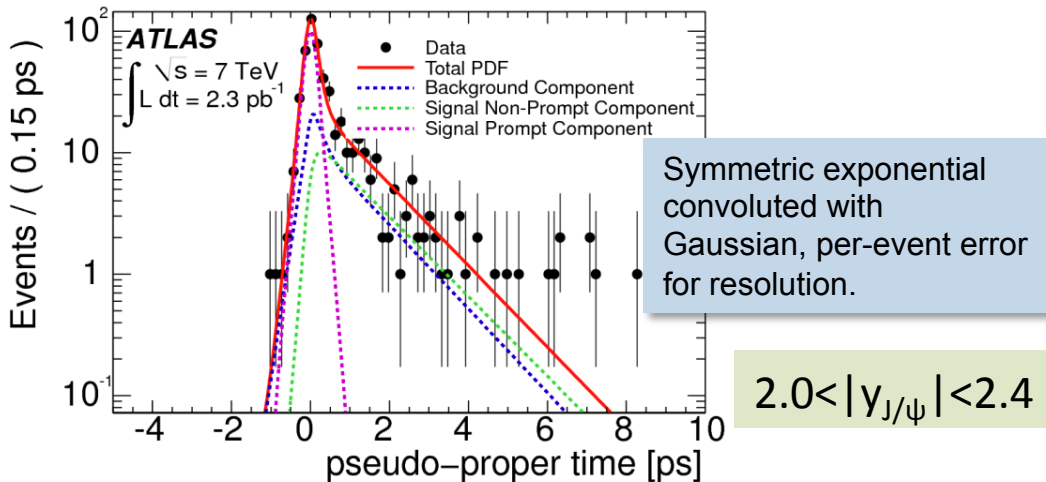
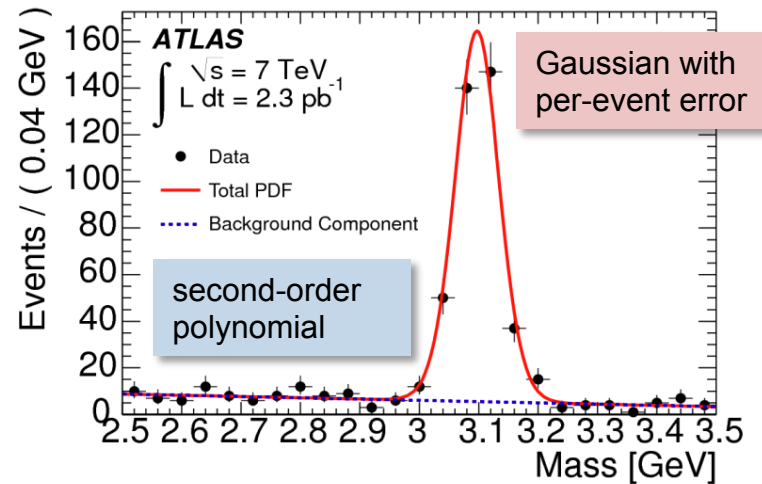
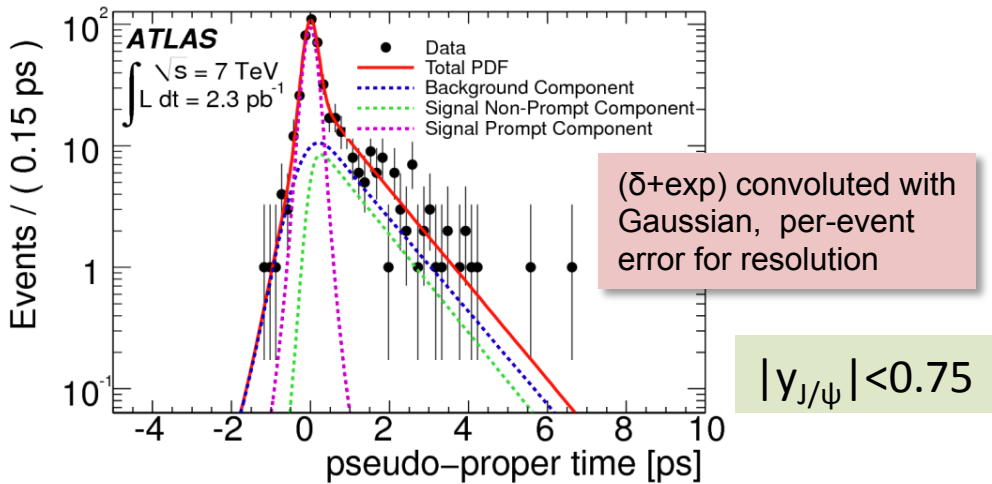
- J/ψ produced within $1.5 < |y| < 2$ and $p_T > 1$ GeV , maximum range of p_T .

$$Br(J/\psi \rightarrow \mu^+\mu^-)\sigma(pp \rightarrow J/\psi X; 1.5 < |y_{J/\psi}| < 2, p_T^{J/\psi} > 1 \text{ GeV}) \\ = 510 \pm 70(\text{stat.}) \pm 120(\text{syst.}) \pm 130(\text{spin}) \pm 20(\text{lumi.}) \text{ nb.}$$

Non-prompt J/ ψ fraction: Simultaneous fit

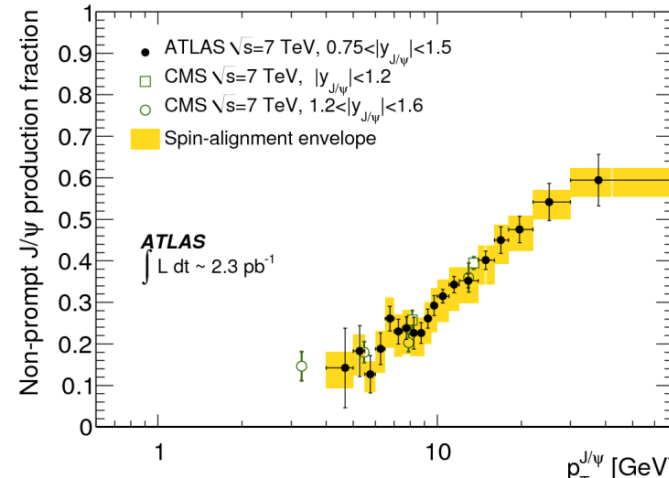
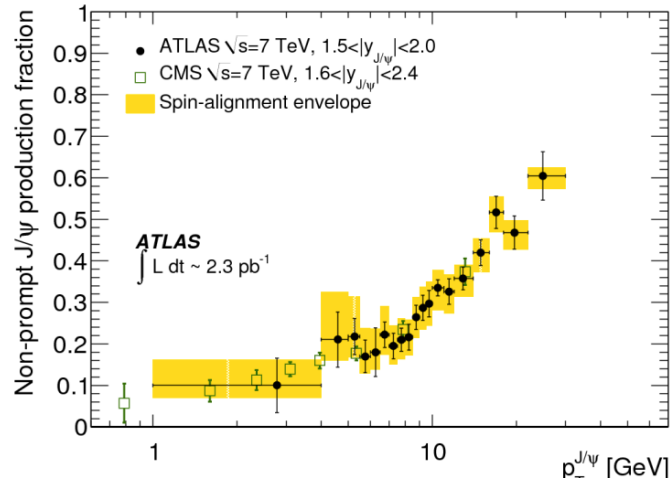
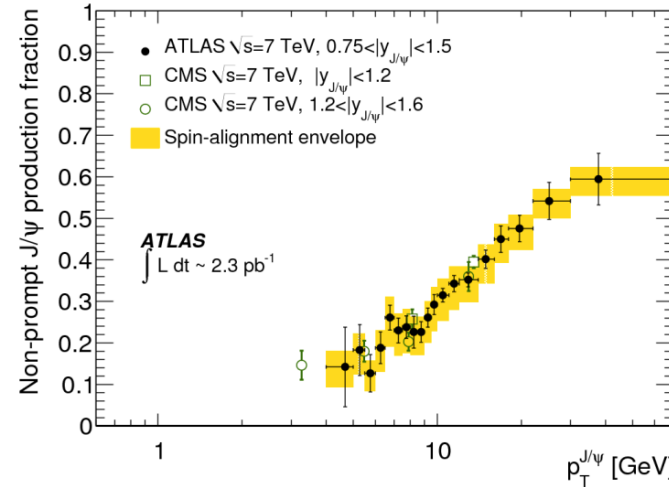
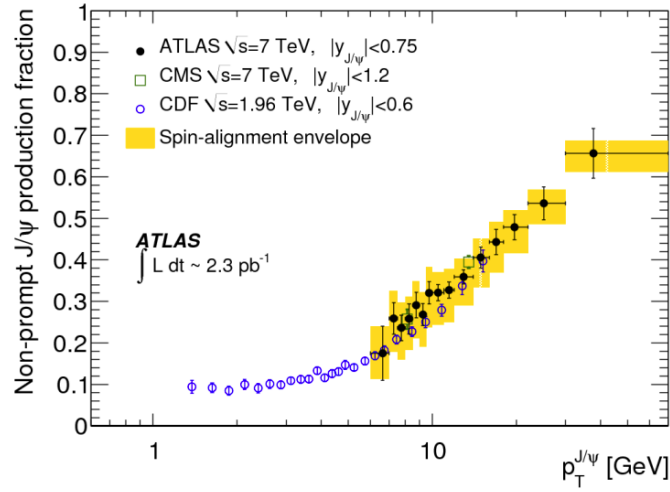
$$\tau = \frac{L_{xy} m_{\text{PDG}}^{\text{J}/\psi}}{p_T^{\text{J}/\psi}}$$

Simultaneous unbinned maximum likelihood fit on invariant mass and pseudo-proper time distribution.



Non-prompt J/ψ production fraction

- Strong pT dependence of the fraction: $\sim 10\%$ at low pT, $\sim 15\%$ at 7GeV, $\sim 70\%$ at the highest accessible pT.
- No significant rapidity dependence and no strong dependence on collision energies.



Cross-sections of non-prompt J/ ψ

The total cross-section for inclusive $J/\psi \rightarrow \mu^+ \mu^-$ production, multiplied by the branching fraction into muons and under the “FLAT” production scenario:

- J/ψ produced within $|y| < 2.4$ and $p_T > 7$ GeV, maximum range of y .

$$Br(J/\psi \rightarrow \mu^+ \mu^-) \sigma(pp \rightarrow B + X \rightarrow J/\psi X; |y_{J/\psi}| < 2.4, p_T^{J/\psi} > 7 \text{ GeV}) \\ = 23.0 \pm 0.6(\text{stat.}) \pm 2.8(\text{syst.}) \pm 0.2(\text{spin}) \pm 0.8(\text{lumi.}) \text{ nb}$$

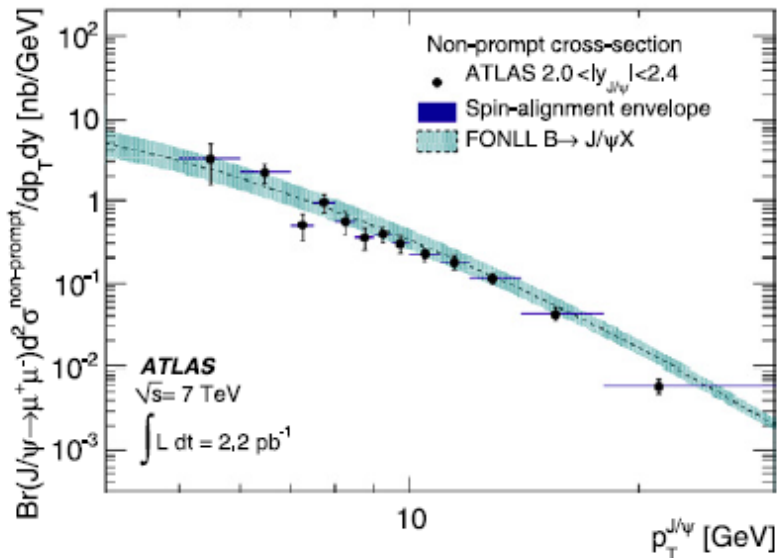
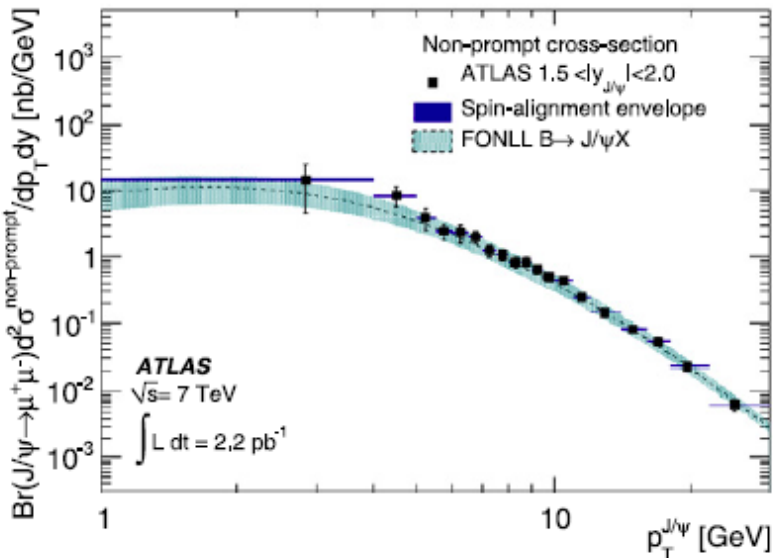
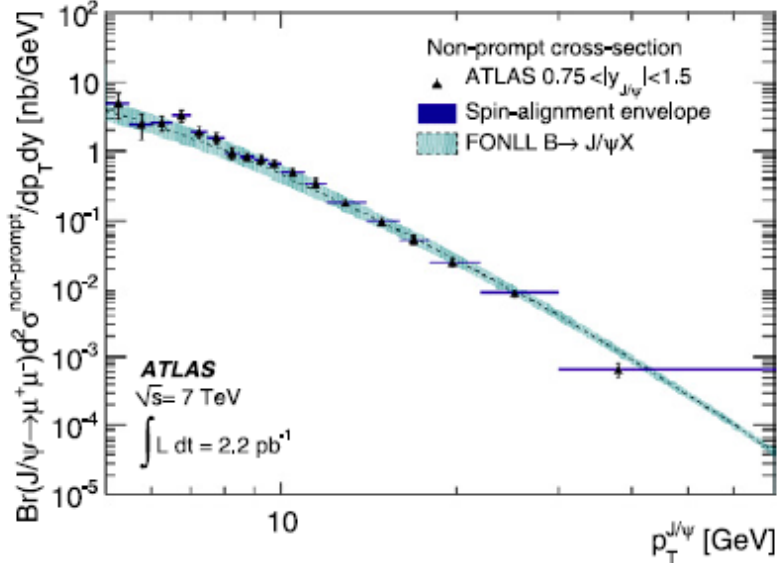
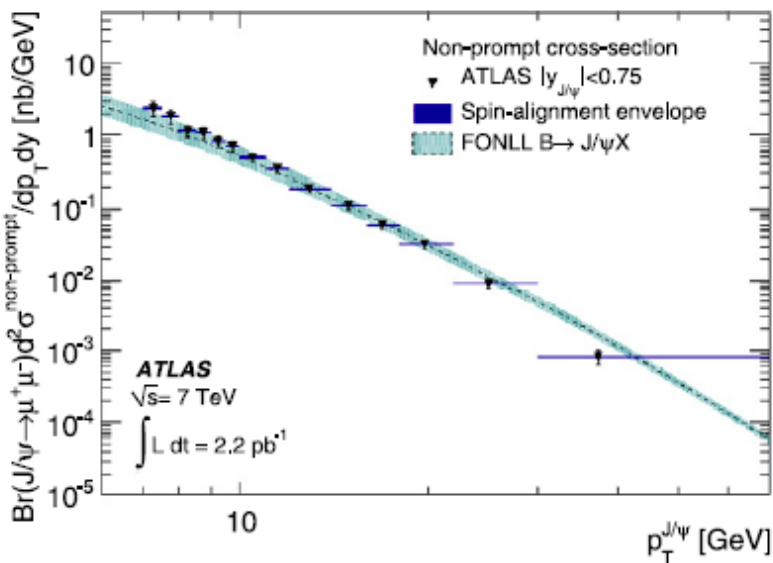
- J/ψ produced within $1.5 < |y| < 2$ and $p_T > 1$ GeV , maximum range of p_T .

$$Br(J/\psi \rightarrow \mu^+ \mu^-) \sigma(pp \rightarrow B + X \rightarrow J/\psi X; 1.5 < |y_{J/\psi}| < 2, p_T^{J/\psi} > 1 \text{ GeV}) \\ = 61 \pm 24(\text{stat.}) \pm 19(\text{syst.}) \pm 1(\text{spin}) \pm 2(\text{lumi.}) \text{ nb.}$$

- Compared to Fixed Order Next-to-Leading-Log (FONLL), good agreement.
(see next slide)

p_T (GeV)	$\langle p_T \rangle$ (GeV)	$\frac{d^2\sigma^{non-prompt}}{dp_T dy} \cdot Br(J/\psi \rightarrow \mu^+ \mu^-)$ [nb/GeV]	$0.75 < y < 1.5$	FONLL prediction		
		Value	$\pm(\text{stat.})$	$\pm(\text{syst.})$	$\pm(\text{spin})$	
5.0–5.5	5.3	4.9	± 1.7	± 1.2	± 0.15	$3.8 \pm^{1.6}_{1.1}$
9.5–10.0	9.8	0.65	± 0.06	± 0.07	± 0.02	$0.56 \pm^{0.20}_{0.13}$
30.0–70.0	38.0	0.0007	± 0.0001	± 0.0001	± 0.0000	$0.0007 \pm^{0.0001}_{0.0001}$

Cross-sections of non-prompt J/ψ



Cross-sections of prompt J/ψ

The total cross-section for inclusive $J/\psi \rightarrow \mu^+\mu^-$ production, multiplied by the branching fraction into muons and under the “FLAT” production scenario:

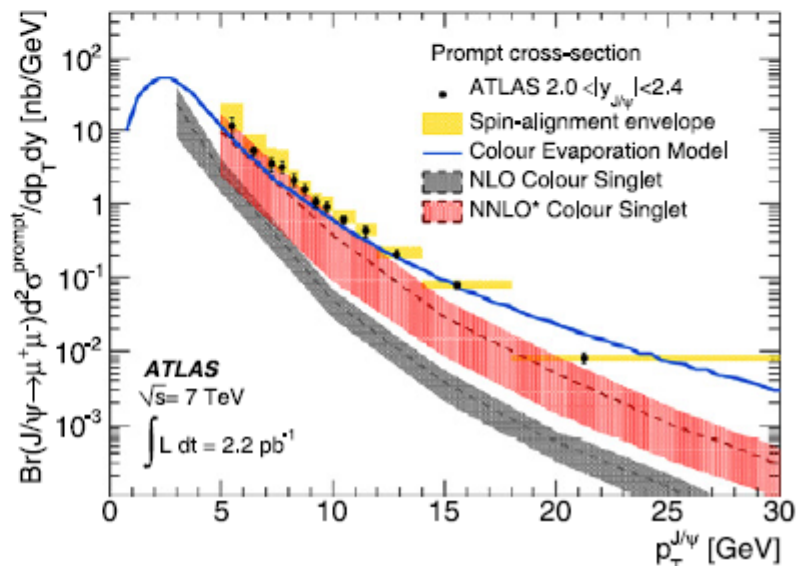
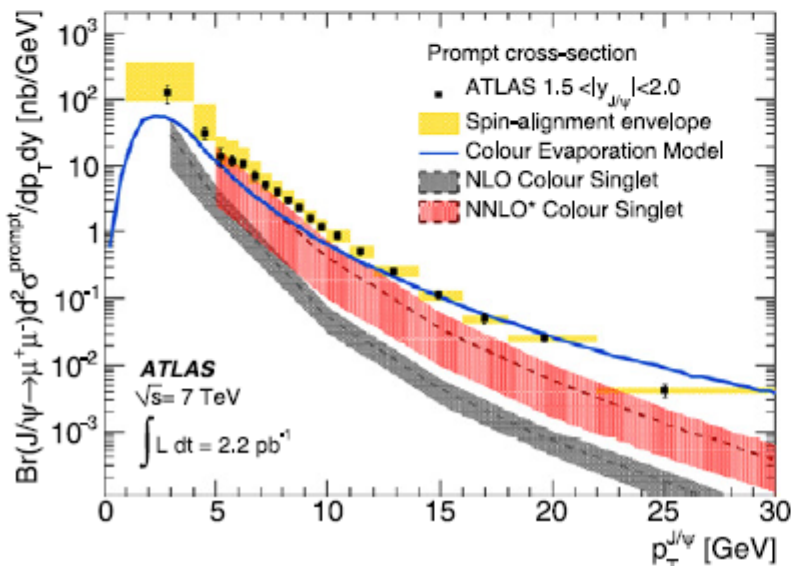
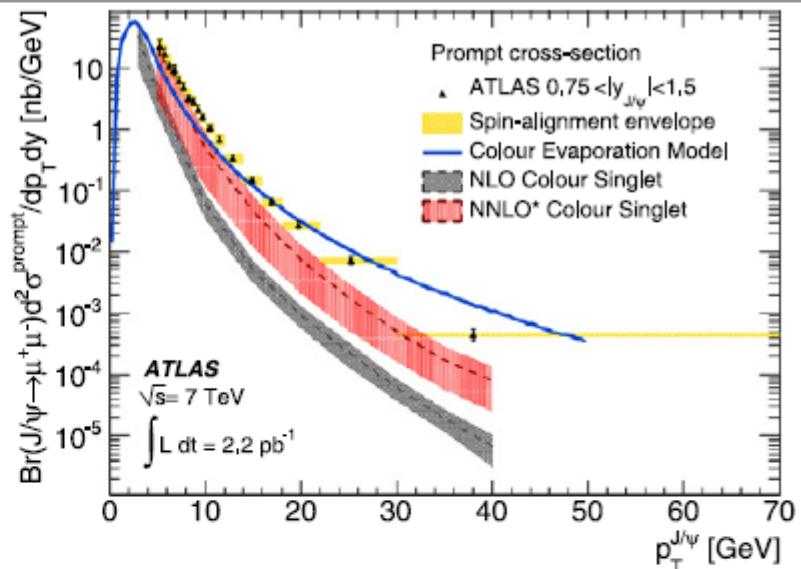
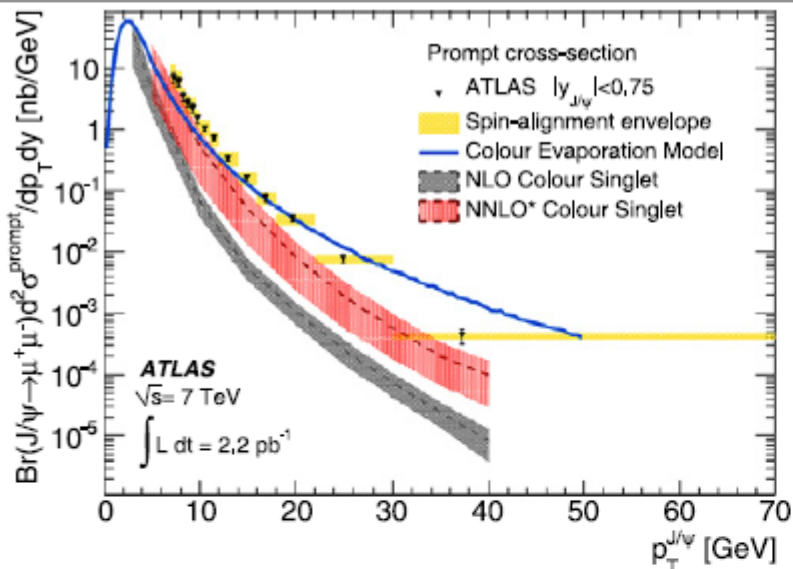
- J/ψ produced within $|y| < 2.4$ and $p_T > 7$ GeV, maximum range of y .

$$Br(J/\psi \rightarrow \mu^+\mu^-)\sigma(pp \rightarrow \text{prompt } J/\psi X; |y| < 2.4, p_T > 7 \text{ GeV}) \\ = 59 \pm 1(\text{stat.}) \pm 8(\text{syst.}) \pm 9_6^9 (\text{spin}) \pm 2(\text{lumi.}) \text{ nb}$$

- J/ψ produced within $1.5 < |y| < 2$ and $p_T > 1$ GeV , maximum range of p_T .

$$Br(J/\psi \rightarrow \mu^+\mu^-)\sigma(pp \rightarrow \text{prompt } J/\psi X; 1.5 < |y| < 2, p_T > 1 \text{ GeV}) \\ = 450 \pm 70(\text{stat.}) \pm 90_{110}^{110} (\text{syst.}) \pm 740_{110}^{110} (\text{spin}) \pm 20(\text{lumi.}) \text{ nb.}$$

Cross-sections of prompt J/ψ



*Measurement of the $\Upsilon(1S)$ production
cross-section in pp collisions at $\sqrt{s} = 7\text{ TeV}$
in ATLAS*

Y(1S) production cross-section

- Results were obtained using 1.13 pb^{-1} of the ATLAS detector 2010 data.
- $\Upsilon(1S)$ production:
 - Measured as a function of p_T and y .
 - No spin-alignment uncertainty.

$$\frac{d^2\sigma}{dp_T dy} \times \text{BR}(\Upsilon(1S) \rightarrow \mu^+ \mu^-) = \frac{N_{\Upsilon(1S)}}{\int \mathcal{L} dt \times \Delta p_T \times \Delta y},$$

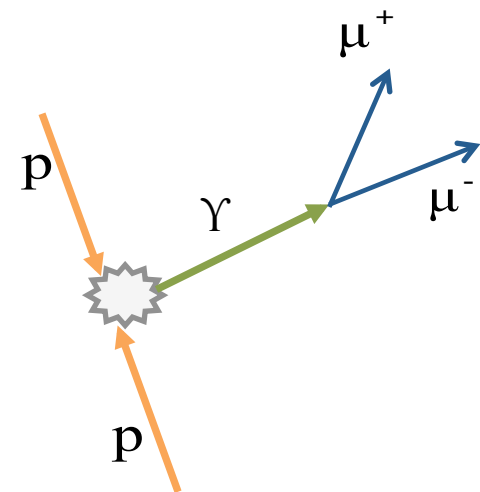
- Weight is evaluated from the single-muon trigger and reconstruction efficiencies. All efficiency factors are determined directly from the data.

$$w = 1/\varepsilon_{\mu\mu} \quad \varepsilon_{\mu\mu} = \varepsilon_{\text{trig}} \varepsilon_{\text{reco}}$$

- Results are compared to various theoretical predictions.

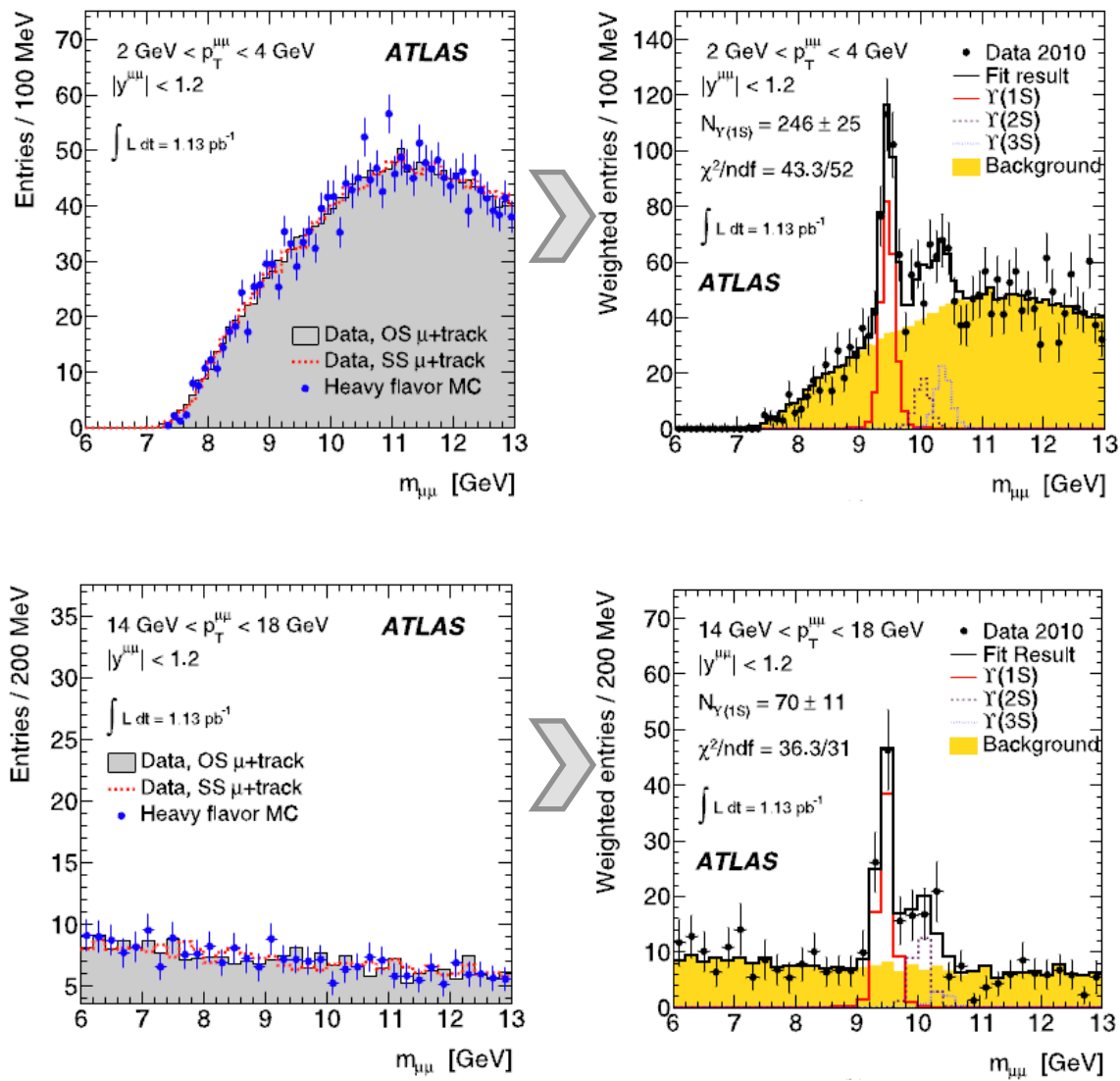
Trigger, events and candidates selection

- Trigger:
 - Single muon trigger with a threshold of $p_T > 4$ GeV.
 - Two offline muons are required with $p_T > 4$ GeV and $|\eta| < 2.5$.
- Selection criteria:
 - Opposite charged Di-muon pair reconstructed.
 - At least 3 tracks associated with primary vertex.
 - At least one muon to be Combined.
 - Tracks: Pixel hits > 0 , SCT hits > 5
 - $|d_0| < 150 \mu\text{m}$ and $|z_0| \sin\theta < 1.5 \text{ mm}$ for γ produced promptly.

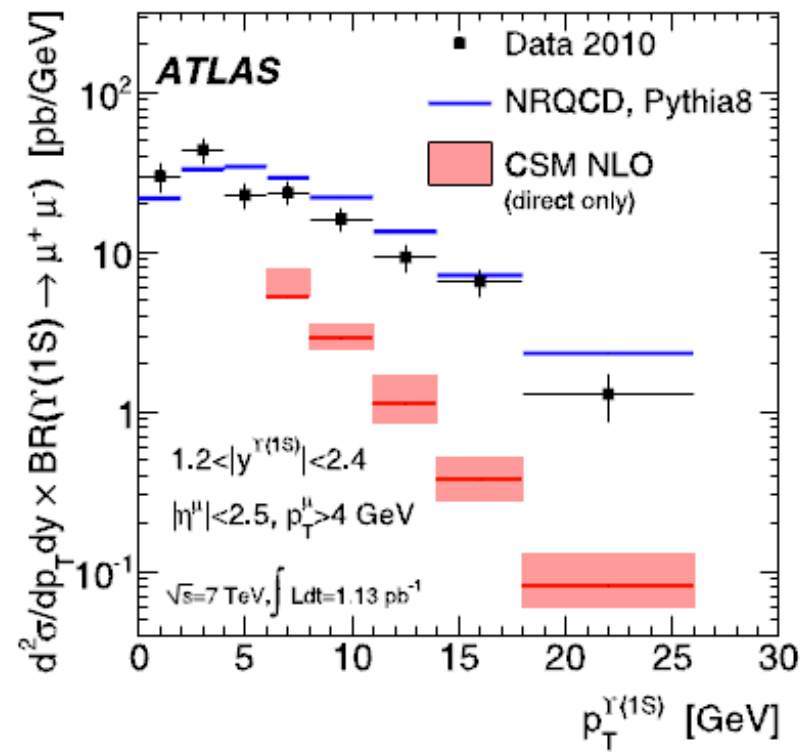
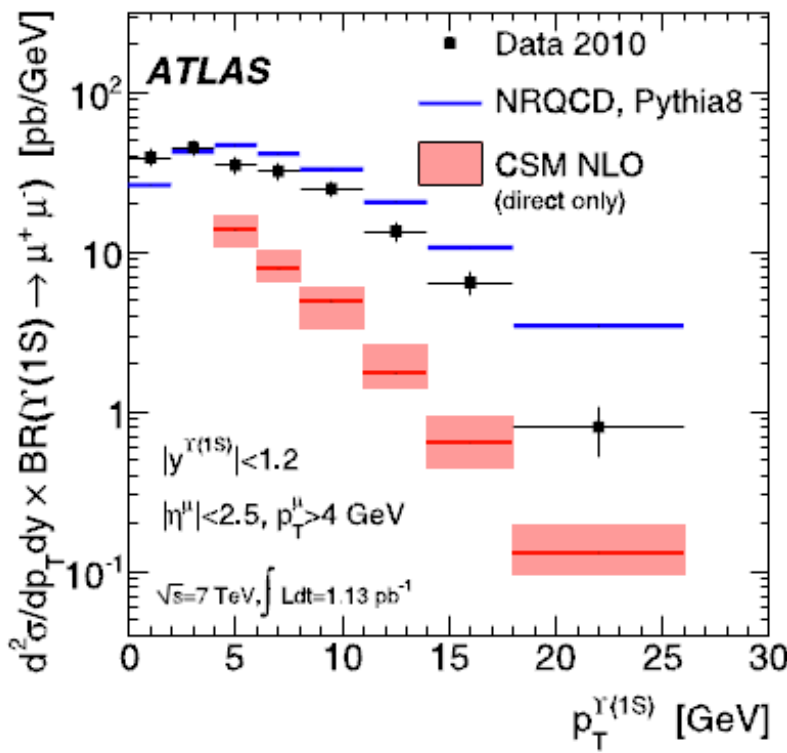


$\Upsilon(1S)$ production: Unbinned maximum likelihood fit

- Background depends on the ($p_T - y$) bins.
- **Signal Model:** from MC
 - Independent for each resonance peak.
 - Resolution adjusted to reflect data.
 - Separation of mass peaks are fixed to world average.
- **Background model:** from data
 - Same selection cuts applied.
 - $\mu + \text{OS track}, \mu + \text{SS track}$, MC give results in agreement (systematic uncertainty).



$\Upsilon(1S)$ production cross-section

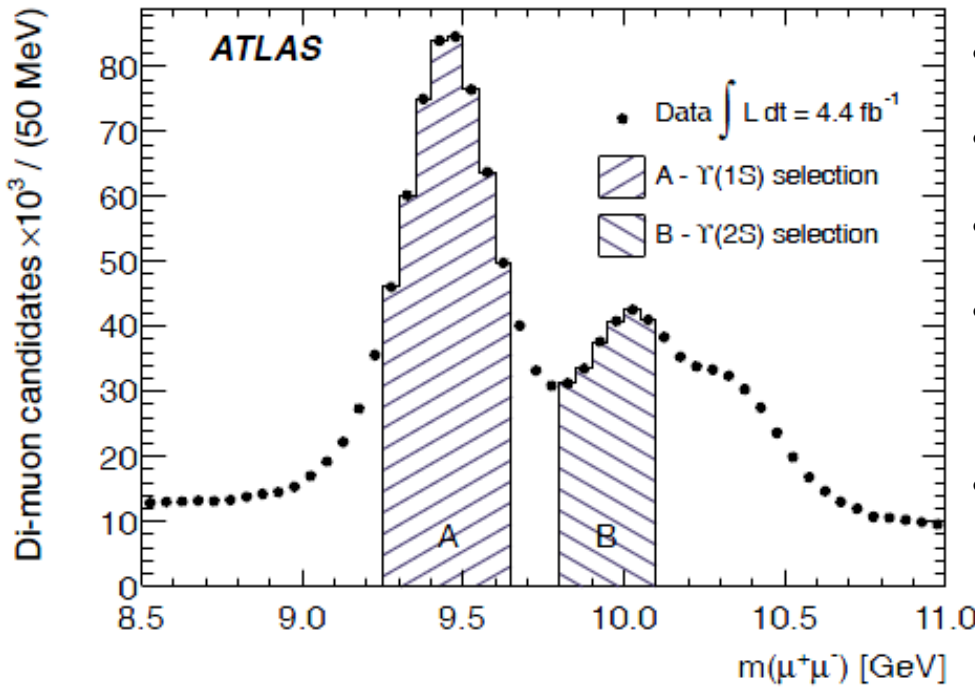


- The typical uncertainty is about 10–15% at low p_T and 35% at high p_T and is dominated by the statistical precision of the data.
- Exceed the NLO prediction, no feed-down from higher mass bound states have been included and higher order correction is needed.
- Agree with NRQCD prediction but different in the shape of the p_T spectrum of about a factor of two.

Observation of a New χ_b State in Radiative Transitions to $Y(1S)$ and $Y(2S)$ at ATLAS

Observation of $\chi_b(3P)$ State

- b quarkonium $\chi_b(1P)$, $\chi_b(2P)$ states have been reconstructed with the ATLAS detector through the radiative decay modes $\chi_b(nP) \rightarrow Y(1S)\gamma$ and $\chi_b(nP) \rightarrow Y(2S)\gamma$.
- $\chi_b(3P)$ has not been previously observed.
- 4.4 fb^{-1} 2011 data.



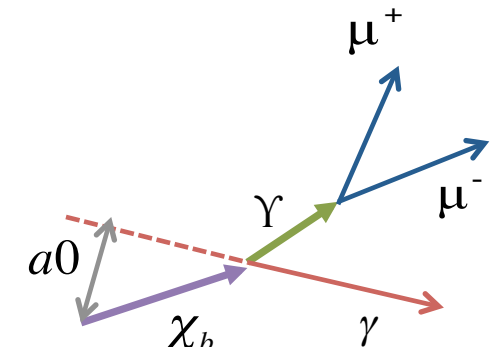
$Y(1S,2S) \rightarrow \mu^+ \mu^-$

- Opposite charged Di-muon pair.
- Both muons are of “combined” type.
- Tracks: $p_T > 4 \text{ GeV}$, $|\eta| < 2.3$.
- Di-muon: $p_T > 12 \text{ GeV}$, $|\eta| < 2.0$, $\chi^2/\text{n.d.o.f} < 20$.
- The asymmetric mass window for $Y(2S)$ is chosen to reduce contamination from the $Y(3S)$ peak and continuum background contributions.

Photon reconstruction

Converted photons:

- Two oppositely charged ID tracks intersecting at a conversion vertex.
- Opening angle constrained to be zero.
- $p_T > 500\text{MeV}$, $|\eta| < 2.3$, SCT hits ≥ 4 , $a_0 < 2\text{mm}$.
- The conversion vertex is required to be at least 40 mm from the beam axis and vertex probability > 0.01 .



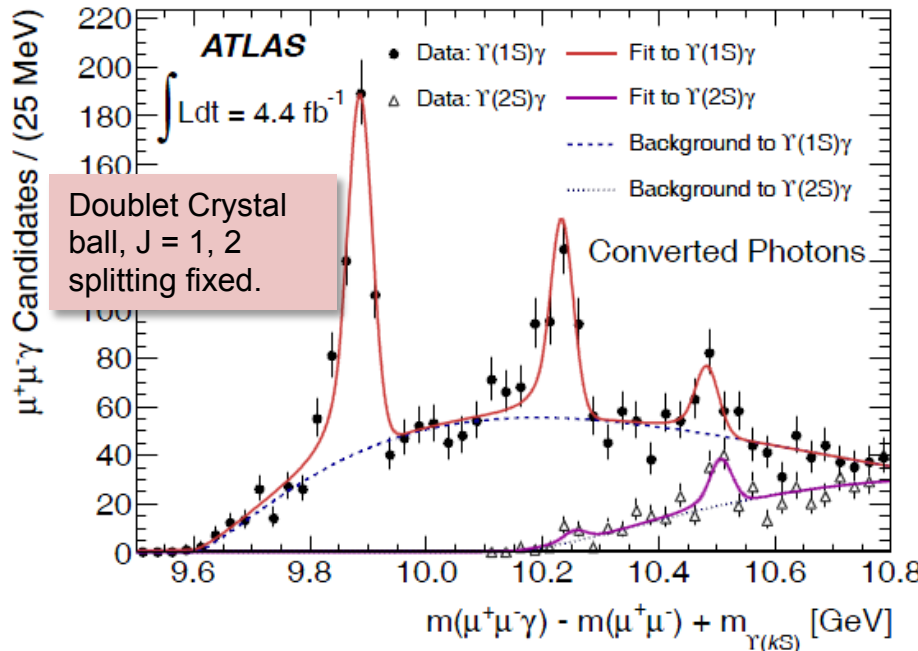
Unconverted photons:

- Photon transverse energy $> 2.5 \text{ GeV}$ (prevent $\chi_b(2P,3P) \rightarrow Y(2S)\gamma$ decays)
- Limit on the fraction of the energy deposit in the Hadronic Calorimeter.
- Transverse width of the shower is required to be consistent with the narrow shape expected for an EM shower.
- Photon polar angle correction is determined using the measurement of the photon direction from the longitudinal segmentation of the calorimeter and the constraint from the di-muon vertex position.
- $|\eta| < 2.37$.

Observation of $\chi_b(3P)$ State

$\Delta m = m(\mu^+\mu^-\gamma) - m(\mu^+\mu^-)$ to minimize the effect of $\gamma \rightarrow \mu^+\mu^-$ resolution.

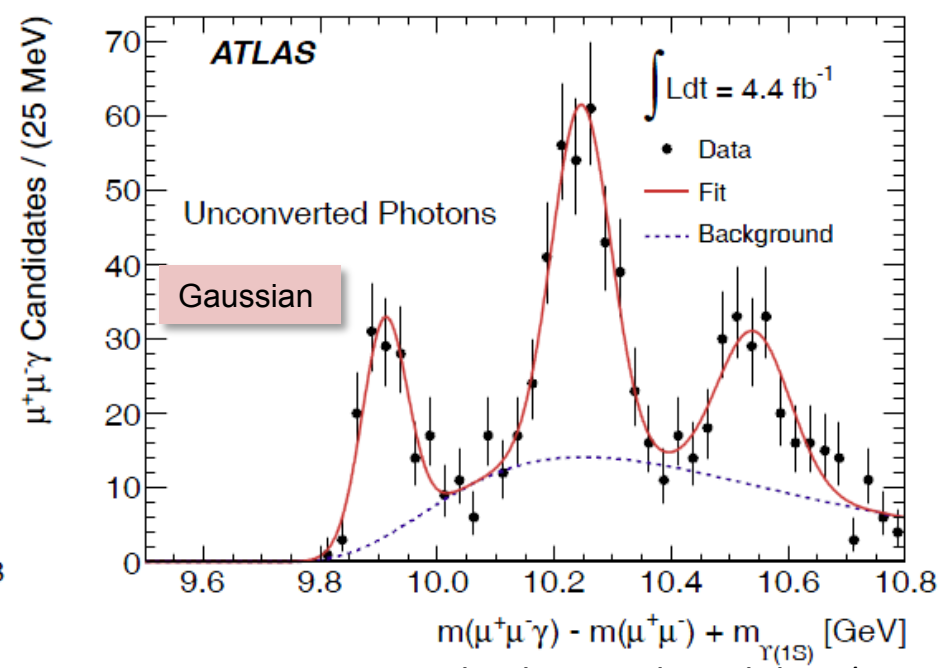
Converted photons: $p_T(\mu^+\mu^-) > 12$ GeV.



Systematic uncertainty: unknown relative normalizations of $J = 1$ and $J = 2$ states (± 5 MeV) and background modeling (± 5 MeV).

New structure observed at mass of $10.530 \pm 0.005(\text{stat.}) \pm 0.009(\text{syst.})$ GeV, it is interpreted as the radiative decay of the $\chi_b(3P)$ state.

Unconverted photons: $p_T(\mu^+\mu^-) > 20$ GeV.



Systematic uncertainty: background modeling (± 21 MeV) and photon energy scale ($\pm 2\%$).

Summary

- Measurement of the J/ψ production differential cross-sections with the largest p_T range: $1 \text{ GeV} \sim 70 \text{ GeV}$, $|\eta| < 2.4$.
 - Inclusive J/ψ production cross-sections, good agreement with CMS.
 - Prompt J/ψ fraction measured, strong dependence on p_T but not on η and collision energy.
 - FONLL can describe non-prompt J/ψ production well.
- Measurement of the $Y(1S)$ production cross-section for $p_T > 4 \text{ GeV}$ and $|\eta| < 2.5$.
 - Can not be fully described by theory → further understanding of the complex mechanisms that govern quarkonium production is needed.
- First observation of the new $\chi_b(3P)$ state at ATLAS.

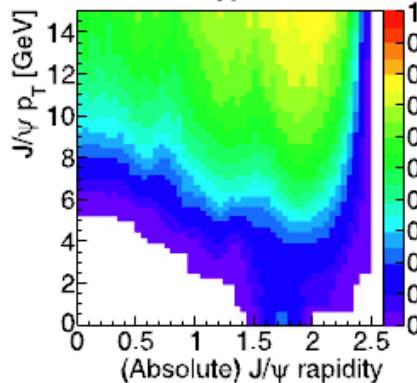
Backup

Inclusive J/ ψ production: Spin-alignment

Angular distribution for the decay:

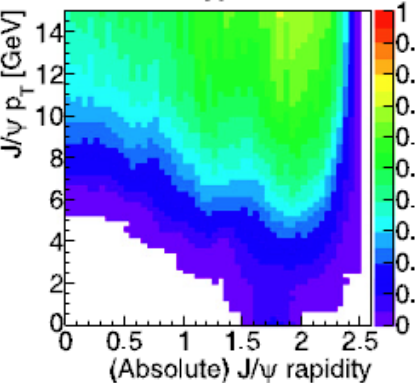
$$\frac{d^2N}{d \cos \theta^* d\phi^*} \propto 1 + \lambda_\theta \cos^2 \theta^* + \lambda_\phi \sin^2 \theta^* \cos 2\phi^* + \lambda_{\theta\phi} \sin 2\theta^*$$

Polarisation hypothesis FLAT



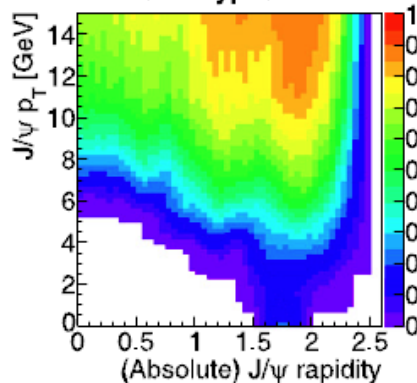
(a) $\lambda_\theta = \lambda_\phi = \lambda_{\theta\phi} = 0$

Polarisation hypothesis T+



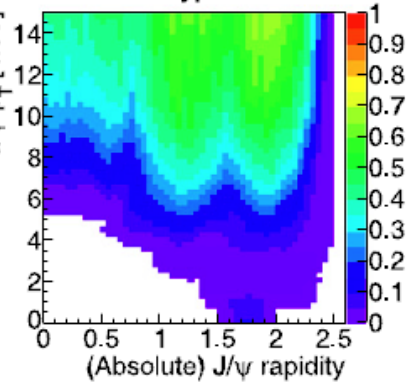
(b) $\lambda_\theta = +1, \lambda_\phi = \lambda_{\theta\phi} = 0$

Polarisation hypothesis LONG



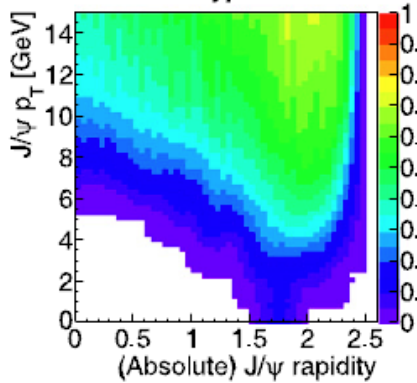
(c) $\lambda_\theta = -1, \lambda_\phi = \lambda_{\theta\phi} = 0$

Polarisation hypothesis T++



(d) $\lambda_\theta = +1, \lambda_\phi = +1, \lambda_{\theta\phi} = 0$

Polarisation hypothesis T+-



(e) $\lambda_\theta = +1, \lambda_\phi = -1, \lambda_{\theta\phi} = 0$

